Investigating thermal donors in n-type Cz silicon with carrier density imaging

Yu Hu, Hendrik Schøn, Eivind Johannes Øvrelid, Øyvind Nielsen, and Lars Arnberg

Citation: AIP Advances **2**, 032169 (2012); doi: 10.1063/1.4754276
View online: http://dx.doi.org/10.1063/1.4754276
View Table of Contents: http://scitation.aip.org/content/aip/journal/adva/2/3?ver=pdfcov
Published by the AIP Publishing

Articles you may be interested in

Light-induced degradation in n-type Czochralski silicon by boron-doping and thermal donor compensation
J. Appl. Phys. **112**, 084509 (2012); 10.1063/1.4759245

Investigating minority carrier trapping in n-type Cz silicon by transient photoconductance measurements
J. Appl. Phys. **111**, 053101 (2012); 10.1063/1.3689786

Influence of net doping, excess carrier density and annealing on the boron oxygen related defect density in compensated n-type silicon
J. Appl. Phys. **110**, 063708 (2011); 10.1063/1.3633492

Lifetime-degrading boron-oxygen centres in p-type and n-type compensated silicon
J. Appl. Phys. **110**, 063515 (2011); 10.1063/1.3609069

Influence of heterogeneous profiles in carrier density measurements with respect to iron concentration measurements in silicon
J. Appl. Phys. **105**, 114903 (2009); 10.1063/1.3138805

Cross-pollinate.
Submit your computational article to *CiSE*.

All article content, except where otherwise noted, is licensed under a Creative Commons Attribution 3.0 Unported license. See: http://creativecommons.org/licenses/by/3.0/
Downloaded to IP: 129.241.191.163 On: Mon, 21 Sep 2015 13:19:31

AIP ADVANCES **2**, 032169 (2012)

Investigating thermal donors in n-type Cz silicon with carrier density imaging

Yu Hu,[1,a] Hendrik Schøn,[2] Eivind Johannes Øvrelid,[3] Øyvind Nielsen,[2] and Lars Arnberg[1]
[1]*Department of Materials Science and Engineering, Norwegian University of Science and Technology, Trondheim, N-7491, Norway*
[2]*NorSun AS, Sommerrogaten 13-15, NO-0255 Oslo, Norway*
[3]*SINTEF Materials Technology, Alfred Getz vei 2B, N-7491, Trondheim, Norway*

(Received 26 June 2012; accepted 5 September 2012; published online 17 September 2012)

A new method to map the thermal donor concentration in silicon wafers using carrier density imaging is presented. A map of the thermal donor concentration is extracted with high resolution from free carrier density images of a silicon wafer before and after growth of thermal donors. For comparison, free carrier density mapping is also performed using the resistivity method together with linear interpolation. Both methods reveal the same distribution of thermal donors indicating that the carrier density imaging technique can be used to map thermal donor concentration. The interstitial oxygen concentration can also be extracted using the new method in combination with Wijaranakula's model. As part of this work, the lifetime at medium injection level is correlated to the concentration of thermal donors in the as-grown silicon wafer. The recombination rate is found to depend strongly on the thermal donor concentration except in the P-band region. *Copyright 2012 Author(s). This article is distributed under a Creative Commons Attribution 3.0 Unported License*. [http://dx.doi.org/10.1063/1.4754276]

I. INTRODUCTION

Cz silicon is generally enriched with interstitial oxygen (O_i) and thermal donors (TDs) form during the cooling process mainly in the temperature range of 400–500°C.[1] TDs are believed to be clusters of oxygen atoms forming during the early stages of oxygen aggregation.[2] They introduce two distinct energy levels, E_c-0.075eV and E_c-0.170eV, into the Si forbidden gap.[3] When the dopant density is below 5×10^{15} cm^{-3}, each TD will provide two electrons and TDs are thus double donors. In this case, the TD concentration in n-type silicon can be calculated as [TDs] = $(n-N_D)/2$ where n is the free carrier density in the as-grown silicon and N_D is the donor (phosphorus) concentration.[4]

The formation and the properties of TDs have been widely investigated.[5] They can change the resistivity of silicon wafers, influence majority carrier transport properties,[6] and act as traps for minority carrier leading to abnormally high lifetime at low injection levels.[7] The TD concentration in silicon wafers can be calculated from the resistivity measured by four-point probe method before and after TD growth.[4,8] If the sample under investigation is scanned, a map of the TD concentration can be acquired. It should be mentioned that the majority carrier mobility μ has to be considered for this method.[9] In the present paper, a new method independent on, μ, is introduced to map the TD concentration in silicon wafers based on the carrier density imaging (CDI) technique. A modified model has been presented recently that is capable of predicting the majority carrier mobility with good accuracy in p-type compensated silicon.[10] Uncertainties in the model remain for n-type compensated silicon.[10] However, these uncertainties can be avoided by using this new method based on CDI. According to the method introduced by Veirman *et al.*,[9] a map of O_i concentration

[a]Author to whom correspondence should be addressed. Electronic mail: yu.hu@material.ntnu.no

 © Author(s) 2012

All article content, except where otherwise noted, is licensed under a Creative Commons Attribution 3.0 Unported license. See: http://creativecommons.org/licenses/by/3.0/
Downloaded to IP: 129.241.191.163 On: Mon, 21 Sep 2015 13:19:31

can be derived from the TD concentration distribution. This can be used to help study the formation of oxygen-related extended defects such as oxygen precipitates and oxygen induced stacking faults (OiSF).[11] However, it is not straightforward concerning the mapping of the O_i concentration since the TD generation may be affected by high degrees of boron-phosphorus compensation that can lead to false O_i mapping. By using the new method, a map can be obtained in several minutes with a spatial resolution of around 350μm not taking into account the time for thermal annealing.

CDI is a lifetime measurement technique based on IR absorption or emission of free carriers in silicon wafers.[12,13] It can work in two different modes, absorption mode or emission mode, depending on the set-up of the equipment.[12] In our experimental setup, the sample is placed on an temperature-controlled mirror which can be heated to 100°C. This mirror is coated with aluminum giving a high reflectivity of IR radiation. A CCD camera that is sensitive to the mid-IR wavelength in the range of 3.7-5μm is used to image the IR emission from the silicon wafer. In this work, an IR topography image that contains the reflected IR radiation and the emission signals from free carriers present in the silicon wafer without illumination is used to map the TD concentration. The net signal from the investigated silicon wafer is obtained by subtracting the background signal of the camera. In order to reduce the error due to variation of background temperature, we image the background signal each time after measuring samples rather than use the same image of background signal. The free carrier density (FCD) can then be derived after calibration of the camera signal. The IR absorption by free carriers in the measured wafer can be neglected in our CDI since it works in emission mode at a temperature in the range of 60-70°C.[12] The lifetime is measured under steady-state illumination by two lasers with the wavelength of 940nm and determined by $\tau = \Delta n/g_e$ (where Δn is the excess carrier density and g_e is the generation rate of electron-hole pairs. Δn is obtained by subtracting the FCD of the sample in the dark from the FCD of the sample under illumination).

In this work, the calibration of the camera signal is performed prior to the CDI measurement. By subtracting the FCD map of a wafer after TD growth from that of the wafer before TD growth, the TD concentration is successfully mapped with a high resolution. For comparison, mapping can also be performed by the resistivity method introduced by Veirman el by taking into account the effect of TDs on the majority carrier mobility.[9] A good agreement of the TD distributions is obtained between the two methods. The map of TD concentration obtained by the new method is then applied to derive the map of O_i concentration using Wijaranakula's model.[14] At the end, the TD concentration in an as-grown silicon wafer is mapped by the CDI technique and correlated to the lifetime in a neighboring wafer to investigate the influence of TDs on lifetime. It is found that TDs play a significant role in the recombination process in the n-type Cz silicon wafers.

II. EMISSION CALIBRATION FOR CDI AT 70°C

The calibration was performed using seven p-type Cz wafers of different doping levels. In order to increase the emission signal of free carriers, the silicon wafer was heated to 70°C. The camera signal was then plotted as a function of doping concentration × thickness of the wafer. The results are shown in Fig. 1 and a linear fit was obtained with the slope of $m = 12.547\times10^{-13}$ digits · cm^2. The FCD in a measured wafer can be determined by the following equation,[13]

$$n(x, y) = \frac{digits_T(x, y) - digits_B(x, y)}{mW\sigma} \tag{1}$$

where $digits_T(x,y)$ is the camera signal with wafer on the mirror and $digits_B(x,y)$ is the camera signal from the background without wafer on the mirror, W is the thickness of the investigated wafer, and σ is a calibration factor considering the fact that p-type wafers were used in the calibration process and thus only IR emission of holes was measured.[15] Since only IR emission of electrons is measured in the n-type silicon samples, the calibration factor σ is given by $\sigma = \frac{\alpha_n}{\alpha_p} = \frac{1\times10^{-18}\lambda^2 n}{2.7\times10^{-18}\lambda^2 p} = \frac{1}{2.7}$, where $\alpha_{n,p}$ is the absorption coefficient for electron and hole free carrier respectively; λ is the wavelength of the IR radiation; n and p are the density of free elections and holes respectively.

All article content, except where otherwise noted, is licensed under a Creative Commons Attribution 3.0 Unported license. See: http://creativecommons.org/licenses/by/3.0/
Downloaded to IP: 129.241.191.163 On: Mon, 21 Sep 2015 13:19:31

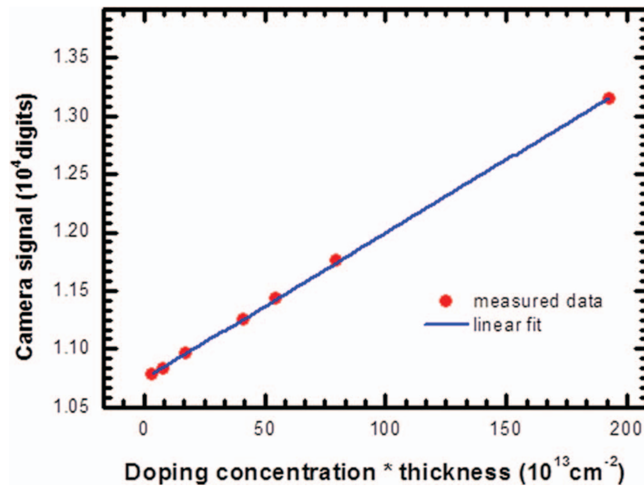

FIG. 1. Emission calibration at 70°C using seven p-type Cz silicon wafer with different doping level.

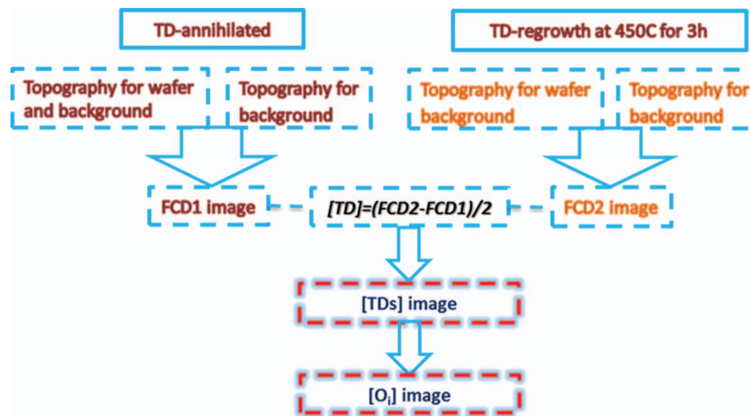

FIG. 2. Procedure of mapping the TD concentration using CDI topography.

III. EXPERIMENTAL

The Cz crystal used in the present study was grown in an argon atmosphere. It was phosphorus-doped and $< 100 >$-oriented. The feedstock was Siemens solar grade silicon produced by a tier 1 vendor. The average body growth rate of ∼1.5 mm/min is state-of-the-art in industrial CZ silicon for photovoltaic applications, giving vacancy-rich growth. Two axial wafers were sliced from the top part of the Cz ingot to obtain a broad distribution of high oxygen concentration. Both wafers are mirror-polished on both surfaces. In this work, TD annihilation was performed in a rapid thermal annealing (RTA) furnace at 800°C for 10s with a ramping rate of 50°C/s and a cooling rate of 30°C/s. This process has been demonstrated to effectively dissolve TDs in silicon wafers.[1] The lowest resistivity measured on the annealed wafer is $8.5\Omega \cdot$cm well above the limit value of $1\Omega \cdot$cm (5×10^{15} cm^{-3}). All the TDs in the as-grown silicon wafers are therefore double TDs. In order to control TD growth process, the TDs was annihilated in one wafer at 800°C for 10s and regrown at 450°C for 3h. IR topography was acquired by CDI before and after TD regrowth. The procedure for mapping the TD concentration is shown in Fig. 2.

For comparison, the TD concentration was also mapped using the resistivity method. Point-by-point measurements were performed manually at room temperature before and after the TD growth, and the TD concentration was calculated according to the method introduced by Veirman *et al.*.[9]

All article content, except where otherwise noted, is licensed under a Creative Commons Attribution 3.0 Unported license. See: http://creativecommons.org/licenses/by/3.0/
Downloaded to IP: 129.241.191.163 On: Mon, 21 Sep 2015 13:19:31

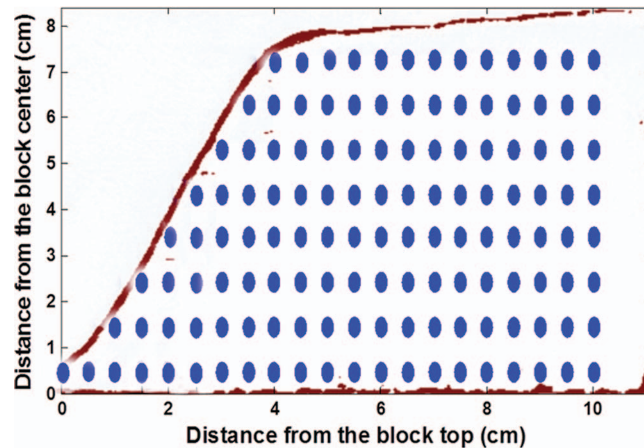

FIG. 3. Sketch of positions for resistivity measurement.

Fig. 3 shows the measured positions on the wafer. Linear interpolation between these measurement points was performed to make comparison with the results from the CDI technique easier.

The O_i concentration was estimated from the TD concentration based on the model of Wijaranakula.[9,14] As the TD concentration was calculated from the emission signal that is unrelated to the free carrier mobility, the effect of TDs on the majority mobility doesn't have to be taken into account in the CDI method.

IV. RESULTS AND DISCUSSION

A. FCD imaging and TD concentration imaging with CDI

Fig. 4(a) illustrates a homogenous FCD (phosphorus) concentration in an axial wafer after TD annihilation. However, significant changes are observed in the wafer after TD regrowth as shown in Fig. 4(b) and two regions of high FCD are revealed in the figure. One is located at around 3cm from the top of the block and extends to 3cm away from the axis. The other is located in the range of 4-8cm from the top of the block and extends to about 6cm away from the axis. It is reasonable to assume that the high FCD in the two regions resulted from ionization of thermal donors. The TD concentration was mapped according to the procedure illustrated in Fig. 2 and the result is shown in Fig. 4(c). Two regions of high TD concentration can be observed at the same positions as the two prominent regions in Fig. 4(b). The highest TD concentration is 1.7×10^{15} cm^{-3}.

In the edge regions of the wafer very high CDI-signals are measured. This is due to the fact that the CDI measurement is sensitive to the surface conditions of the investigated sample, and a rough surface with scratches can result in a signal overestimation.[16] If the surface conditions of an investigated wafer are different from those of the calibration wafers, the calculated TD concentration will differ from the true TD concentration. In order to perform a correct calculation, a new calibration has to be carried out using calibration wafers with similar surface condition as the investigated wafer or an additional surface correction is required.[16]

B. Mapping of TD concentration by resistivity measurement

When TDs are absent in the wafer, an image of homogenous phosphorus concentration is revealed by both the CDI method and the resistivity method (see Fig. 5) with an average phosphorus concentration at around 5×10^{14} cm^{-3}. After introducing TDs into the wafer, the image of the TD concentration shows qualitatively the same distribution but the concentration determined by the CDI method is higher than that by the resistivity method. Despite the difference exists between the TD concentration mapped by the two methods, a good agreement is achieved on the distribution of TD concentration.

All article content, except where otherwise noted, is licensed under a Creative Commons Attribution 3.0 Unported license. See: http://creativecommons.org/licenses/by/3.0/
Downloaded to IP: 129.241.191.163 On: Mon, 21 Sep 2015 13:19:31

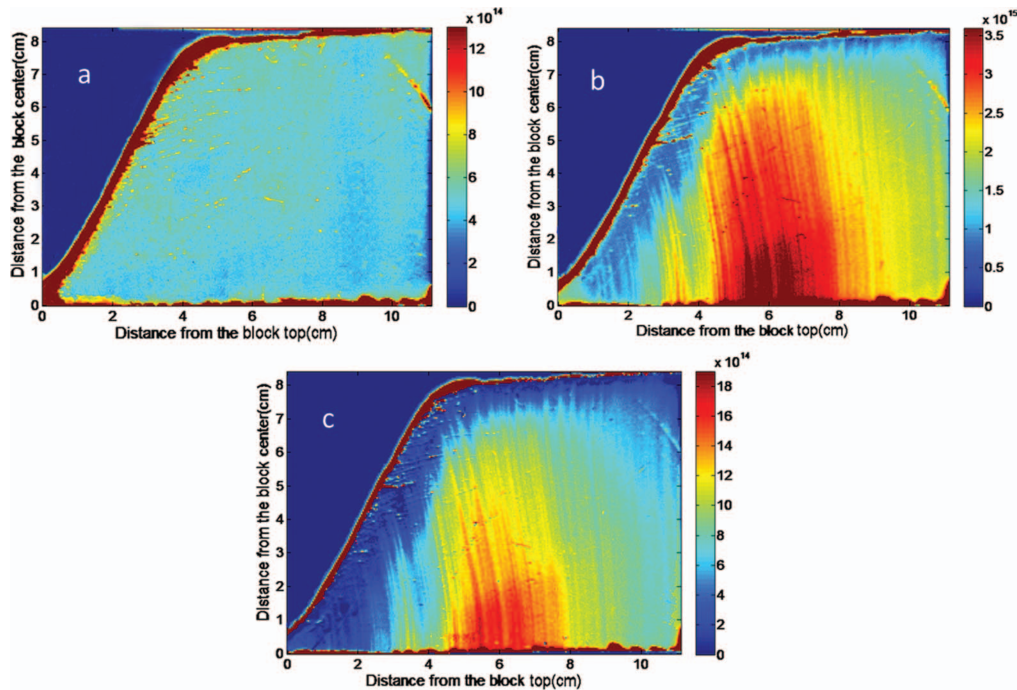

FIG. 4. a) FCD1(cm^{-3}) imaging by CDI at 70°C in a TD-annihilated silicon wafer. b) FCD2 (cm^{-3}) imaging by CDI at 70°C in a TD-regrown silicon wafer. c) [TD] (cm^{-3}) imaging by CDI at 70°C in a TD-regrown silicon wafer.

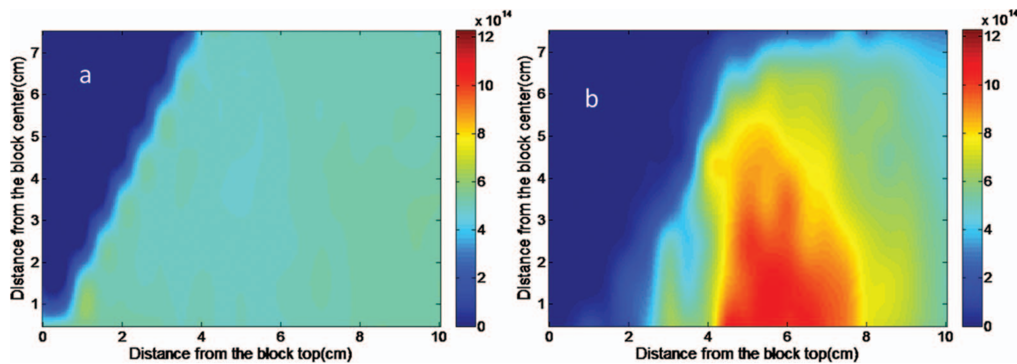

FIG. 5. a) Phosphorous concentration (cm^{-3}) imaging by resistivity measurement in TD-annealed silicon wafer. b) TD concentration (cm^{-3}) imaging in the silicon wafer after TD regrowth.

C. O_i concentration mapping

A super linear relationship between the concentration of TDs and O_i is shown in Fig. 6, illustrating that the TD concentration is an increasing function of O_i concentration. Large differences in the TD concentration corresponds to small differences in the O_i concentration (eg. The TD concentration will increase from $\sim 10^{11}$ cm^{-3} to $\sim 10^{15}$ cm^{-3} if the O_i concentration increase from 10^{17} cm^{-3} to 10^{18} cm^{-3}). Therefore, the two maps of O_i concentrations are more similar to each other than the two maps of TD concentration.

Fig. 7 reveals the O_i concentration in the wafer after TD annihilation rather than the total oxygen concentration. The oxygen particles in the P-band did not dissolve at 800°C and therefore the oxygen from these particles did not contribute to TD growth at 450°C. Higher temperature anneal, such as homogenization anneal for 15min at 1000°C,[17] is required to dissolve grown-in oxide particles and the mapping of the total oxygen concentration could be performed using the same procedure as presented above. As shown in Fig. 7(a), the O_i concentration map with high resolution obtained

All article content, except where otherwise noted, is licensed under a Creative Commons Attribution 3.0 Unported license. See: http://creativecommons.org/licenses/by/3.0/
Downloaded to IP: 129.241.191.163 On: Mon, 21 Sep 2015 13:19:31

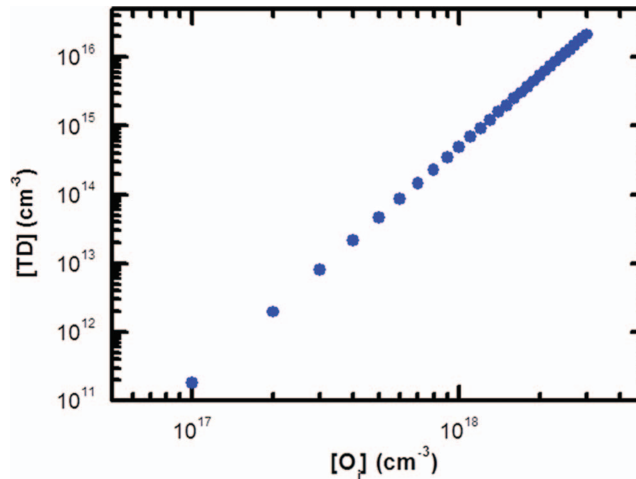

FIG. 6. Dependence of [TD] on [O_i] for silicon wafers annealed at 450°C for 3h based on the model by Wijaranakula.

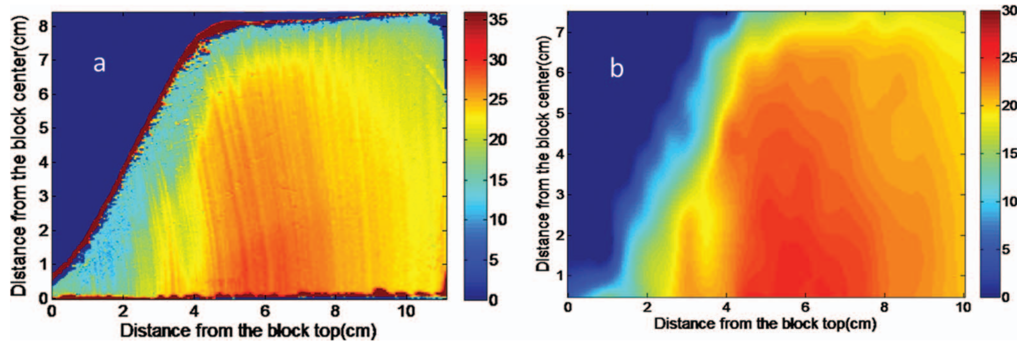

FIG. 7. a) mapping of [O_i] (ppm) with CDI method after annealing at 450°C for 3h. b) [Oi] (ppm) with resistivity method.

by the CDI method reveals an inhomogeneous distribution of O_i and the clearly visible striations are probably oxygen striations. In silicon ingot the oxygen distribution differs from the distribution of the other impurities and the effective segregation coefficient of oxygen is close to one. Oxygen dissolves into the melt from the crucible, and therefore the incorporation of oxygen into the growing crystal is strongly dependent on the melt flow patterns. The unsteady melt flows give rise to unsteady supply of oxygen and the oxygen striations that are thicker than dopant striations.[18]

D. Correlation of lifetime to TD concentration in as-grown silicon

The lifetime was measured on another as-grown wafer by CDI at 60°C with the illumination of 1sun. In order to reduce the influence of surface recombination, the wafer was chemically polished and passivated with a-Si by PECVD according to the process described by Dauwe *et al.*.[19] However, the effective lifetime measured on the passivated wafer is still lower than that measured on the ingot through transient-PCD with the maximum lifetime about 6ms at an excess carrier density of 5×10^{14} cm^{-3}. The higher the bulk lifetime is, the larger the observed difference. As shown in Fig. 8. low lifetimes are obtained at the same positions with the two prominent regions of high TD concentration in Fig. 4(c). Moreover, a narrow blue band is observed with even lower lifetime. This band is called the P-band. It is rich in oxide particles and known as an OiSF-ring after oxidation.[20] These oxide particles are assumed to be active recombination centers. The P-band emerges when the V/G ratio is slightly higher than the $(V/G)_{critical}$ values where V is the growth rate and G is the thermal gradient.[21] It located at the edge of the vacancy defect region. In the P-band the O_i concentration is reduced due to the formation of oxide particles during the crystal cooling process. It was found

All article content, except where otherwise noted, is licensed under a Creative Commons Attribution 3.0 Unported license. See: http://creativecommons.org/licenses/by/3.0/
Downloaded to IP: 129.241.191.163 On: Mon, 21 Sep 2015 13:19:31

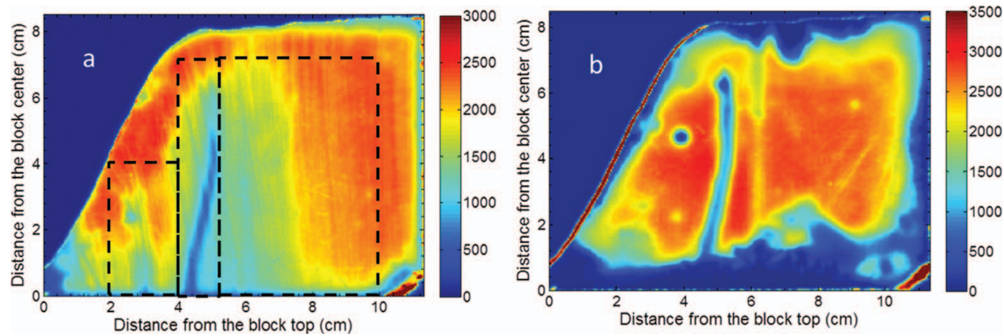

FIG. 8. a) Lifetime (μs) imaging by CDI at 60°C of an as-grown silicon wafer. b) Lifetime (μs) imaging by CDI at 60°C of the silicon wafer after TD annihilation. Data in the areas marked by three dotted frames in Fig. 8(a) are used for correlation shown in Fig. 9(a).

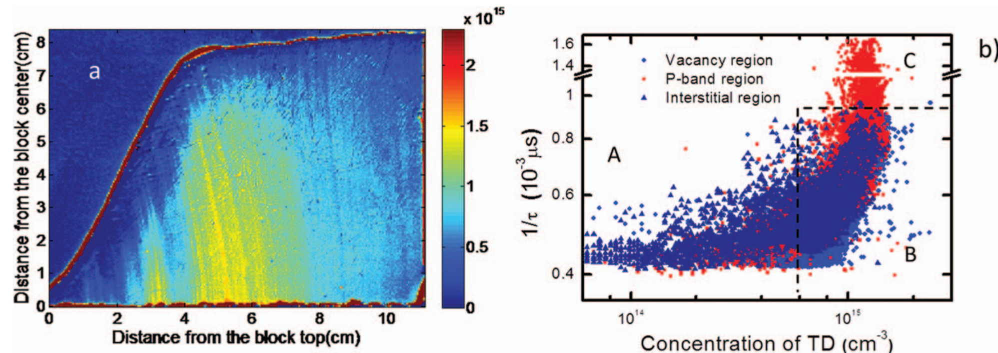

FIG. 9. a) TD concentration (cm^{-3}) imaging by CDI at 70°C in an as-grown silicon wafer. b) Correlation between the TD concentration and the effective lifetime in as-grown silicon wafers. The data were selected from the three regions in the dotted frame as shown in the Fig. 8(a) and the corresponding regions in Fig. 9(a).

that the P-band can still be observed after TD annihilation as shown in Fig. 8(b) since those oxide particles cannot be dissolved at 800°C. However, the lifetime in the two regions increased by a factor of two after TD annihilation indicating that TDs are also active recombination centers, whereas in the wafer periphery the lifetime decreased significantly probably due to contamination during the TD annihilation at 800°C.

In order to investigate the relationship between the lifetime and TDs, three areas were selected in Fig. 8(a) and the corresponding areas in Fig. 9(a). They are marked by three dotted frames as shown in Fig. 8 located in the interstitial region, the P-band region and the vacancy region respectively. The inverse lifetime is plotted as a function of the TD concentration in Fig. 9(b), which shows three different regions revealing different dependence of the inverse lifetime on the TD concentration. In region A, TDs show no obvious influence on the lifetime below 6×10^{14} cm^{-3}. This could be due to insufficient passivation, since the maximum effective lifetime measured on the passivated wafer is lower than the maximum lifetime measured on the ingot. In region B, the inverse lifetime or recombination rate is increasing with the increasing TD concentration and a super linear dependence is observed, indicating that lifetime has degraded in both regions with high TD concentration. However, in region C, the inverse lifetime is distributed at a constant TD concentration. All the data in region C are collected from the P-band region, and therefore it is probably indicating that the dominating recombination centers are oxide particles rather than TDs. Therefore, we can conclude that in the interstitial and the vacancy regions the lifetime should mainly depend on the concentration of TDs or other defects which have the same distribution and thermal stability as TDs, while in the P-band region the dominating recombination centers are oxide particles.

All article content, except where otherwise noted, is licensed under a Creative Commons Attribution 3.0 Unported license. See: http://creativecommons.org/licenses/by/3.0/
Downloaded to IP: 129.241.191.163 On: Mon, 21 Sep 2015 13:19:31

V. CONCLUSION

CDI has been used to map the concentration of TDs and O_i in n-type Cz silicon wafer. It was observed that the TD concentrations mapped through the CDI method was higher than the corresponding values calculated from the resistivity measurements but the same distribution of TD concentration was revealed by both methods. Based on Wijaranakula's model the O_i concentration could be calculated from the CDI measurements. Oxygen striations were clearly revealed in the map. Finally, TD concentrations in an as-grown silicon wafer was imaged and correlated to the effective lifetime measured by CDI. It was found that the effective lifetime was mainly dependent on the TD concentration except in the P-band region and the regions where the maximum effective lifetime are limited by the insufficient passivation, indicating that TDs are active recombination centers in the investigated n-type Cz silicon samples.

ACKNOWLEDGMENTS

This work was performed within the "Monoloco" project co-sponsored by NorSun and the Research Council of Norway. The authors would like to thank Dr. Gaute Stokkan for fruitful discussions and help in setting up the CDI equipment.

[1] Y. Tokuda, N. Kobayashi, A. Usami, Y. Inoue, and M. Imura, Journal of Applied Physics **66**, 3651 (1989).
[2] C. Londos, M. Binns, A. Brown, S. McQuaid, and R. Newman, Applied Physics Letters **62**, 1525 (1993).
[3] M. Bruzzi, D. Menichelli, M. Scaringella, J. Härkönen, E. Tuovinen, and Z. Li, Journal of Applied Physics **99**, 093706 (2006).
[4] P. Wagner and J. Hage, Applied Physics A: Materials Science & Processing **49**, 123 (1989).
[5] A. Ourmazd, W. Schroter, and A. Bourret, Journal of Applied Physics **56**, 1670 (1984).
[6] M. Claybourn and R. Newman, Applied Physics Letters **52**, 2139 (1988).
[7] Y. Hu, H. Schøn, Ø. Nielsen, E. J. Øvrelid, and L. Arnberg, Journal of Applied Physics **111**, 053101 (2012).
[8] J. Veirman, S. Dubois, N. Enjalbert, J. Garandet, D. Heslinga, and M. Lemiti, Solid-State Electronics **54**, 671 (2010).
[9] J. Veirman, S. Dubois, N. Enjalbert, and M. Lemiti, Energy Procedia **8**, 41 (2011).
[10] F. Schindler, M. C. Schubert, A. Kimmerle, J. Broisch, S. Rein, W. Kwapil, and W. Warta, Solar Energy Materials and Solar Cells (In press) (2012).
[11] K. Barraclough, Journal of Crystal Growth **99**, 654 (1990).
[12] M. C. Schubert, J. Isenberg, and W. Warta, Journal of Applied Physics **94**, 4139 (2003).
[13] J. Isenberg, S. Riepe, S. W. Glunz, and W. Warta, Journal of Applied Physics **93**, 4268 (2003).
[14] W. Wijaranakula, Applied Physics Letters **59**, 1608 (1991).
[15] O. Breitenstein, W. Warta, and M. Langenkamp, *Lock-in Thermography: Basics and Use for Evaluating Electronic Devices and Materials* (Springer Berlin Heidelberg, Berlin, Heidelberg, 2010).
[16] M. C. Schubert, S. Pingel, and W. Warta, Journal of Applied Physics **101**, 124907 (2007).
[17] K. F. Kelton, R. Falster, D. Gambaro, M. Olmo, M. Cornara, and P. F. Wei, Journal of Applied Physics **85**, 8097 (1999).
[18] A. Borghesi, B. Pivac, A. Sassella, and A. Stella, Journal of Applied Physics **77**, 4169 (1995).
[19] S. Dauwe, J. Schmidt, and R. Hezel, in *Very low surface recombination velocities on p-and n-type silicon wafers passivated with hydrogenated amorphous silicon films*, New Orleans, 2002 (Proceedings of the 29th IEEE PVSC), p. 1246.
[20] V. Voronkov, Journal of Crystal Growth **310**, 1307 (2008).
[21] V. V. Voronkov and R. Falster, Solid State Phenomena **178**, 3 (2011).

All article content, except where otherwise noted, is licensed under a Creative Commons Attribution 3.0 Unported license. See: http://creativecommons.org/licenses/by/3.0/
Downloaded to IP: 129.241.191.163 On: Mon, 21 Sep 2015 13:19:31